

1

Supporting Information

2 **Functional Thiophene-diketopyrrolopyrrole-based** 3 **Polymer Derivatives as Organic Anode Materials for** 4 **Lithium-ion Batteries**

5 Zichen Xu,^a Shengxian Hou,^a Zhiyou Zhu,^a Pengfei Zhou,^a Li Xue,^a Hongtao Lin,^{*a}

6 Jin Zhou ^a and Shuping Zhuo ^{*a}

7 ^a *School of Chemistry and Chemical Engineering, Shandong University of*

8 *Technology, Zibo 255000, P. R. China. E-mail: linht@sdut.edu.cn*

9 **S1:**

10 **1.1 Materials**

11 Chemicals: sodium tert-butoxide, 2-methyl-2-butanol, 2-Thiophenecarbonitrile
12 and dimethyl succinate were bought from Aladdin to synthesis 3,6-di(thiophen-2-
13 yl)pyrrolo[3,4-c]pyrrole-1,4(2H,5H)-dione (TDPP). TDPP monomers have been
14 synthesized following the reported literature and were carefully purified prior to use in
15 the polymerization reaction [1, 2]. 1-Bromohexane, tert-butyl bromoacetate, N-
16 bromosuccinimide (NBS), N, N-Dimethylformamide (DMF) and chloroform have been
17 purchase from Innochem.

18 **1.2 Monomers synthesis**

19 **3,6-di(thiophen-2-yl)pyrrolo[3,4-c]pyrrole-1,4(2H,5H)-dione (TDPP):** Firstly, 3.43 g

1 sodium tert-butoxide was added in 100 mL boiling flask-3-neck, and then evacuates
2 with N₂ and dropwise adds the mixed solution of 50 mL 2-methyl-2-butanol and 8.4
3 mL 2-Thiophenecarbonitrile. When it is heated to 100~110 °C, add the mixed solution
4 of 5.4 mL dimethyl succinate and 8.0 mL 2-methyl-2-butanol to it dropwise within 1 h
5 and keep the reaction stirred at 110 °C for 24 h. After extraction with acetic acid and
6 washing with deionized water and methanol until the filtrate is clear, pure TDPP was
7 collected as 8.43 g of dark red precipitate representing a yield of 68 %.

8 ***2,5-dihexyl-3,6-di(thiophen-2-yl)pyrrolo[3,4-c]pyrrole-1,4(2H,5H)-dione (TDPP-H):***

9 In 250 mL boiling flask-3-neck, 1.5 g TDPP and 2.07g K₂CO₃ were dissolved in 100
10 mL DMF and stirred in Ar at 120 °C for 1 h. 2.06 g 1-bromohexane was added to it and
11 stirred at 130 °C for 12 h. After the reactant reached room temperature (25 °C), it added
12 200 mL deionized water and was stirred at room temperature for 1 h. Then, using
13 methanol and distilled water to wash the product for multiple times until the filtrate was
14 clear. Finally, the crude product was purified by chromatography, petroleum ether (PE):
15 dichloromethane (DCM) (volume ratio is 4:1) as eluent. After removing solvent under
16 vacuum at 60 °C, pure product TDPP-H was collected as 1.12 g of red precipitate
17 representing a yield of 48 %.

18 **¹H NMR** (400MHz, CDCl₃, ppm): 8.95 (d, J=3.72, 2H), 7.62 (d, J=4.88, 2H), 7.27 (d,
19 J=12.64, 2H), 4.03 (m, 4H), 1.85 (m, 2H), 1.36-1.22 (m, 16H), 0.85 (m, 12H), **MALDI-**
20 **TOF:** 469.19

21 ***di-tert-butyl 2,2'-(1,4-dioxo-3,6-di(thiophen-2-yl)pyrrolo[3,4-c]pyrrole-2,5(1H,4H)-***

22 ***diyl)diacetate (TDPP-TA):*** In 250 mL boiling flask-3-neck, 2.38 g TDPP and 2.73 g

1 K₂CO₃ were dissolved in 100 mL DMF and stirred in Ar at 120 °C for 1 h. 3.86 g tert-
2 butyl bromoacetate and 10 mg 18-crown-6 were added to it and stirred at 120 °C for 20
3 h. After the reactant reached room temperature (25 °C), it was extracted multiple times
4 with saturated saline. Then, using methanol and distilled water to wash the product for
5 multiple times until the filtrate was clear. Finally, the crude product was purified by
6 chromatography, petroleum ether (PE): dichloromethane (DCM) (volume ratio is 1:4)
7 as eluent. After removing solvent under vacuum at 60 °C, pure product TDPP-TA was
8 collected as 1.90 g of purple precipitate representing a yield of 45 %.

9 ¹H NMR (400MHz, CDCl₃, ppm): 8.75 (d, J=3.84, 2H), 7.62 (d, J=4.96, 2H), 7.27 (m,
10 2H), 4.79 (s, 4H), 1.42 (s, 18H), **MALDI-TOF**: 528.14.

11 ***3,6-bis(5-bromothiophen-2-yl)-2,5-dihexylpyrrolo[3,4-c]pyrrole-1,4(2H,5H)-dione***

12 (***TDPP-H-Br***): In 250 mL two-necked flask, 281 mg TDPDO was dissolved in 150 mL
13 anhydrous chloroform and stirred for 15 min at 25 °C with Ar. Then it added 224 mg N-
14 bromosuccinimide (NBS) in three times under dark conditions and the reaction stirred
15 at 25 °C for 48 h. The product was poured into 200 mL methanol and the product was
16 collected by rotary evaporation. Finally, the crude product was purified by
17 chromatography, petroleum ether (PE): dichloromethane (DCM) (volume ratio is 10:1)
18 as eluent. After removing solvent under vacuum at 60 °C, pure product TDPP-H-Br was
19 collected as 255 mg of purple precipitate representing a yield of 68 %.

20 ¹H NMR (400MHz, CDCl₃, ppm): 8.64 (d, J=4.04, 2H), 7.18 (d, J=7.40, 2H), 3.91 (t,
21 J=7.78, 4H), 1.82 (m, 2H), 1.36-1.24 (m, 16H), 0.86 (m, 12H), **MALDI-TOF**: 626.00

22 ***di-tert-butyl 2,2'-(3,6-bis(5-bromothiophen-2-yl)-1,4-dioxopyrrolo[3,4-c]pyrrole-***

1 **2,5(1H,4H)-diyl)diacetate (TDPP-TA-Br):** In 250 mL two-necked flask, 317 mg
2 TDPBA was dissolved in 150 mL anhydrous chloroform and stirred for 15 min at 25
3 °C with Ar. Then it added 224 mg NBS in three times under dark conditions and the
4 reaction stirred at 25 °C for 48 h. The product was poured into 200 mL methanol and
5 the product was collected by rotary evaporation. Finally, the crude product was purified
6 by chromatography, petroleum ether (PE): dichloromethane (DCM) (volume ratio is
7 15:1) as eluent. After removing solvent under vacuum at 60 °C, pure product TDPP-
8 TA-Br was collected as 239 mg of purple precipitate representing a yield of 58 %.

9 **¹H NMR** (400MHz, CDCl₃, ppm): 8.75 (d, J=4.92, 1H), 7.62 (d, J=8.64, 1H), 7.28 (d,
10 J=8.83, 1H), 4.28 (s, 2H), 1.38 (s, 9H). **MALDI-TOF:** 685.95.

11

12

13

14

15

16

17

18

19

20

21

22

23

24

25

26

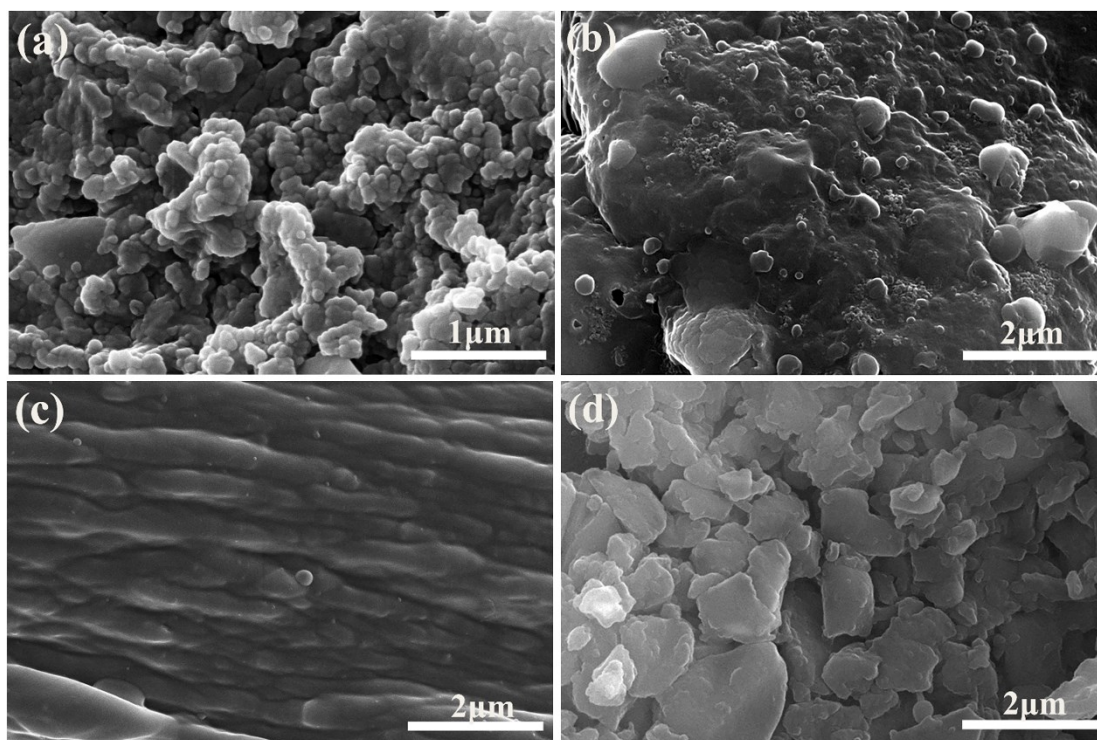
27

28

29

30

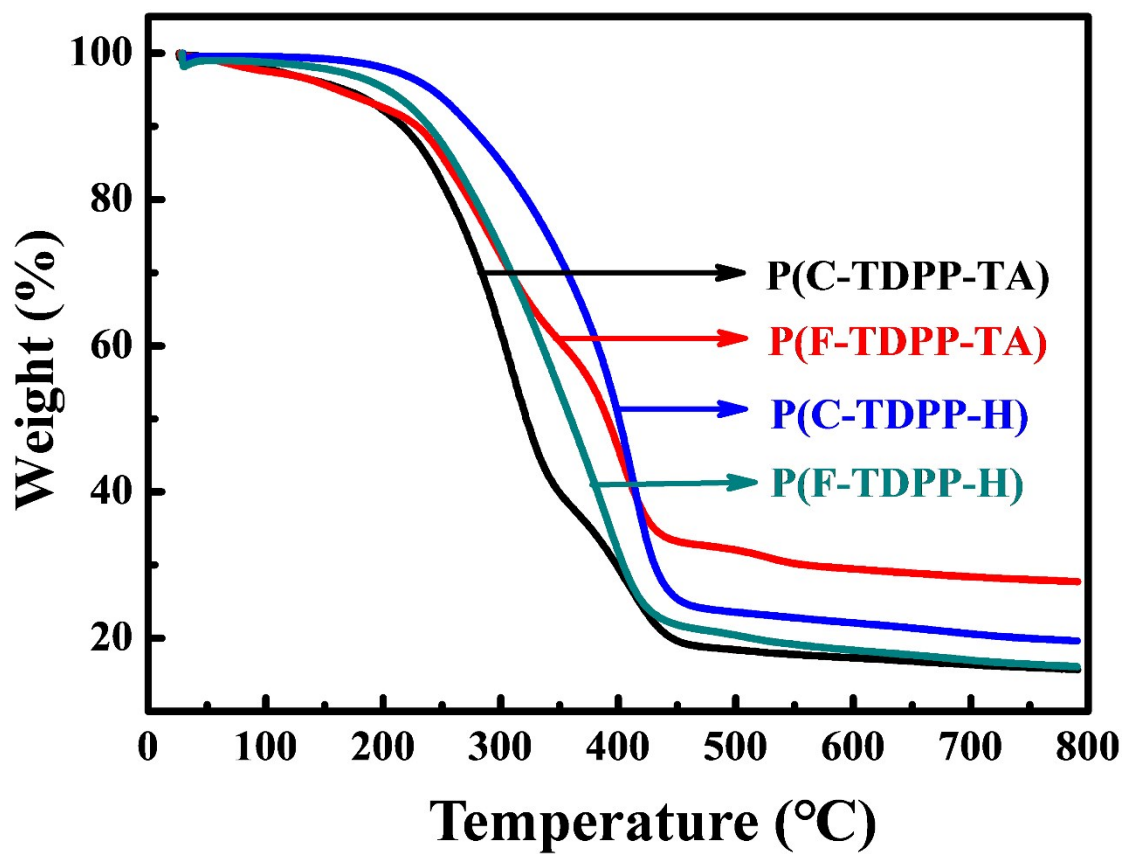
1
2
3 S2



4
5 **Figure S1.** Scanning electron microscopy images of (a) **P(C-TDPP-TA)**, (b) **P(F-**
6 **TDPP-TA)**, (c) **P(C-TDPP-H)** and (d) **P(F-TDPP-H)**.

7 Scanning electron microscopy (SEM) images of polymers can reveal their
8 morphology, crystal characteristics and structural stability. In Figure S1, P(C-TDPP-
9 TA) is aggregated polymer for spherical nanoparticles with a diameter of about 50~100
10 nm, P(F-TDPP-TA) presents membrane morphology on which there are spherical
11 nanostructures with a diameter of about 100~500 nm, P(C-TDPP-H) is a fibrous
12 polymer structure and P(F-TDPP-H) is a few amorphous large granular morphology
13 with a diameter of about 500~2000 nm.

14
15
16
17
18



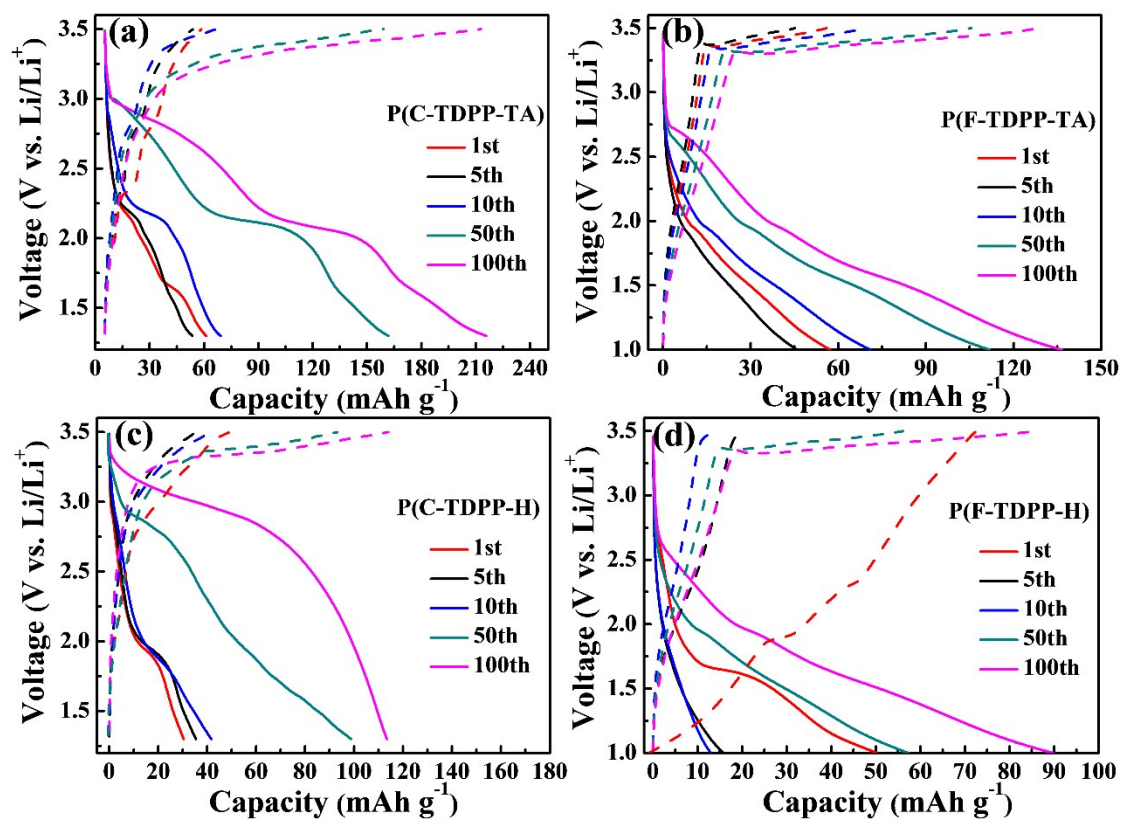
1

2 **Figure S2.** Thermogravimetric analysis curves of **P(C-TDPP-TA)**, **P(F-TDPP-TA)**,
3 **P(C-TDPP-H)** and **P(F-TDPP-H)**. Measurements were carried out under nitrogen
4 atmosphere at a ramp rate of $10^{\circ}\text{C min}^{-1}$.

5

6

7



1

2 **Figure S3.** Galvanostatic charge–discharge profiles of (a) **P(C-TDPP-TA)**, (b) **P(F-**
 3 **TDPP-TA)**, (c) **P(C-TDPP-H)** and (d) **P(F-TDPP-H)** cycled at a current density of
 4 100 mA g⁻¹ in a voltage range of 1.3~3.5 V versus Li/Li⁺.

5

6

7

8

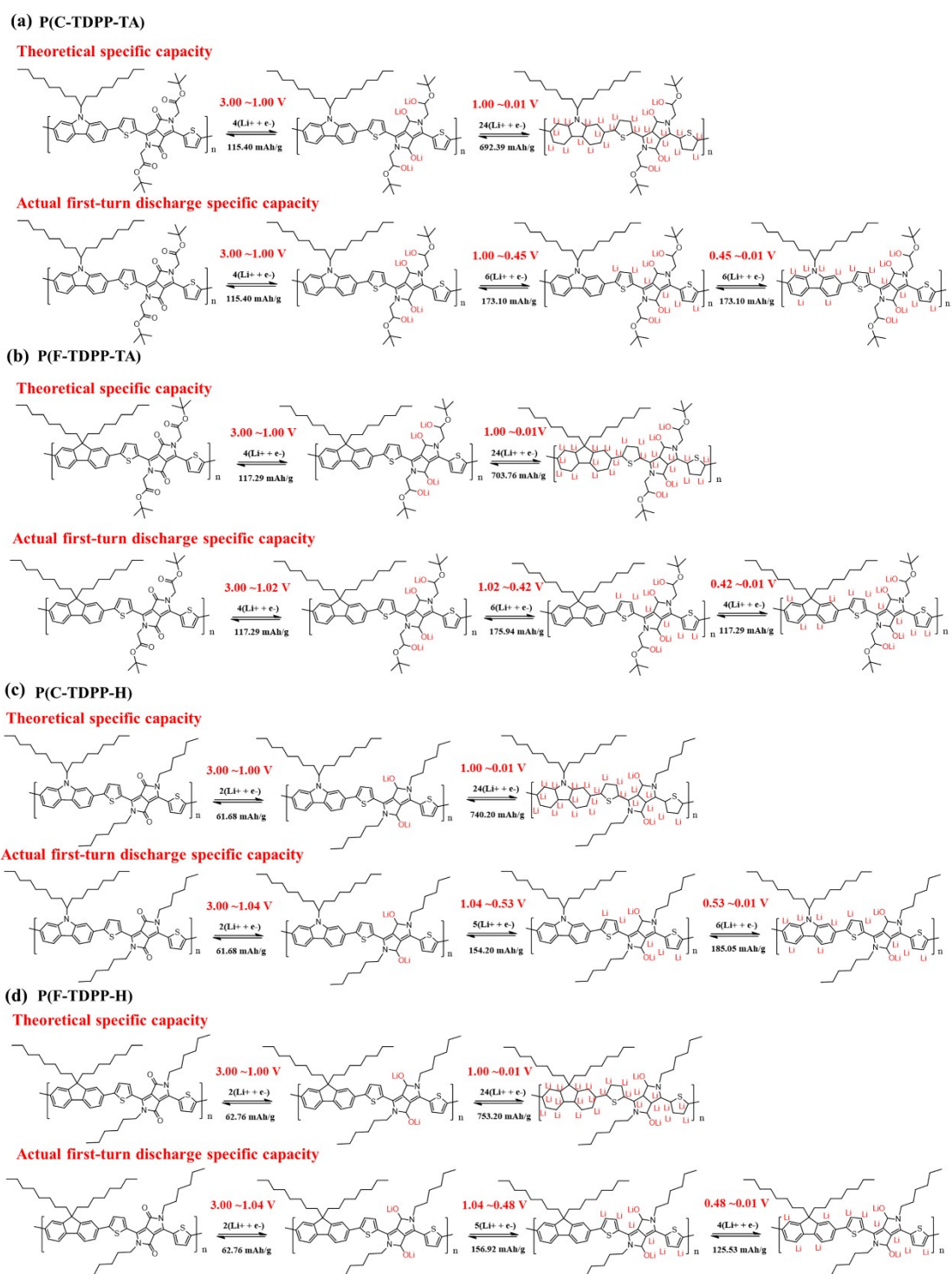
9

10

11

12

13



1

2 **Figure S4.** A plausible electrochemical reaction mechanism of (a) P(C-TDPP-TA), (b)
 3 P(F-TDPP-TA), (c) P(C-TDPP-H) and (d) P(F-TDPP-H) against metallic lithium.

4

5 The calculation formula for the theoretical specific capacity (C_T) of lithium ion battery
 6 electrode materials is as follows:

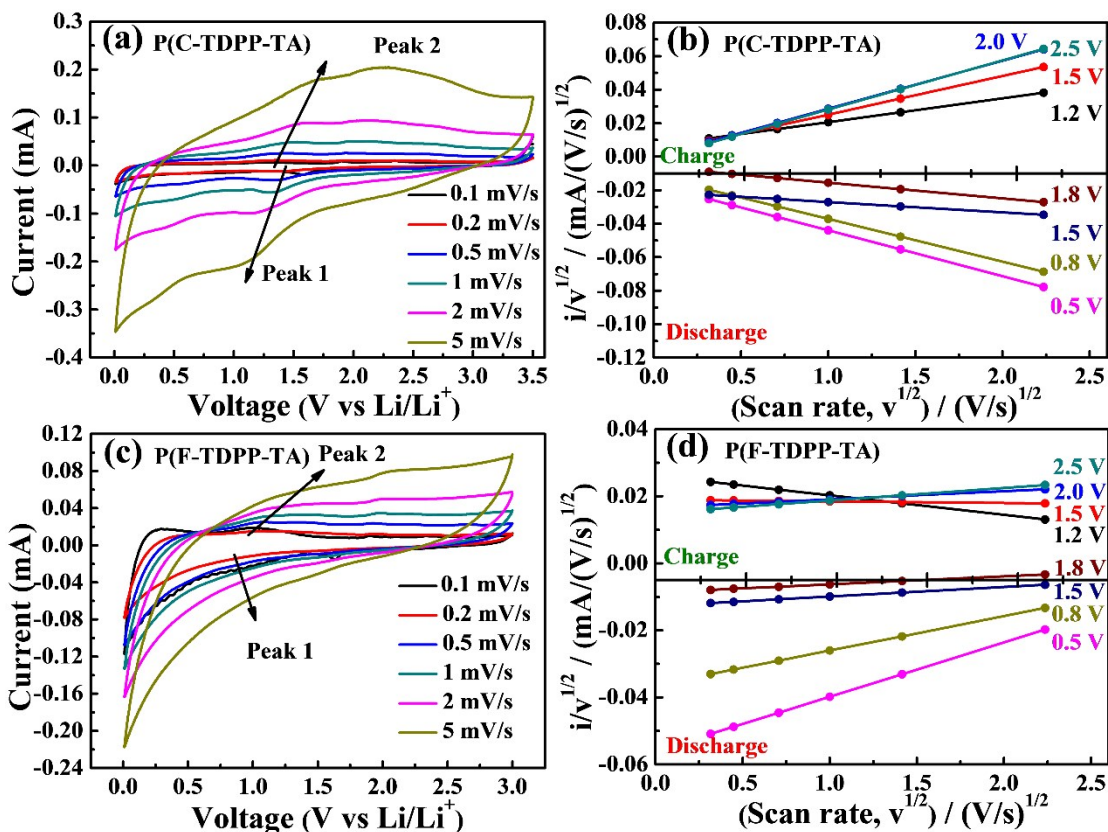
$$7 C_T = n \cdot F / (3.6 \cdot M) \quad (\text{mAh g}^{-1}) \quad (\text{Eq.S1})$$

8 Where F represents Faraday constant ($96485.3383 \pm 0.0083 \text{ C mol}^{-1}$), n (mol) is number

1 of lithium insertion and M (g mol^{-1}) represents the relative mass fraction of the electrode
2 material.

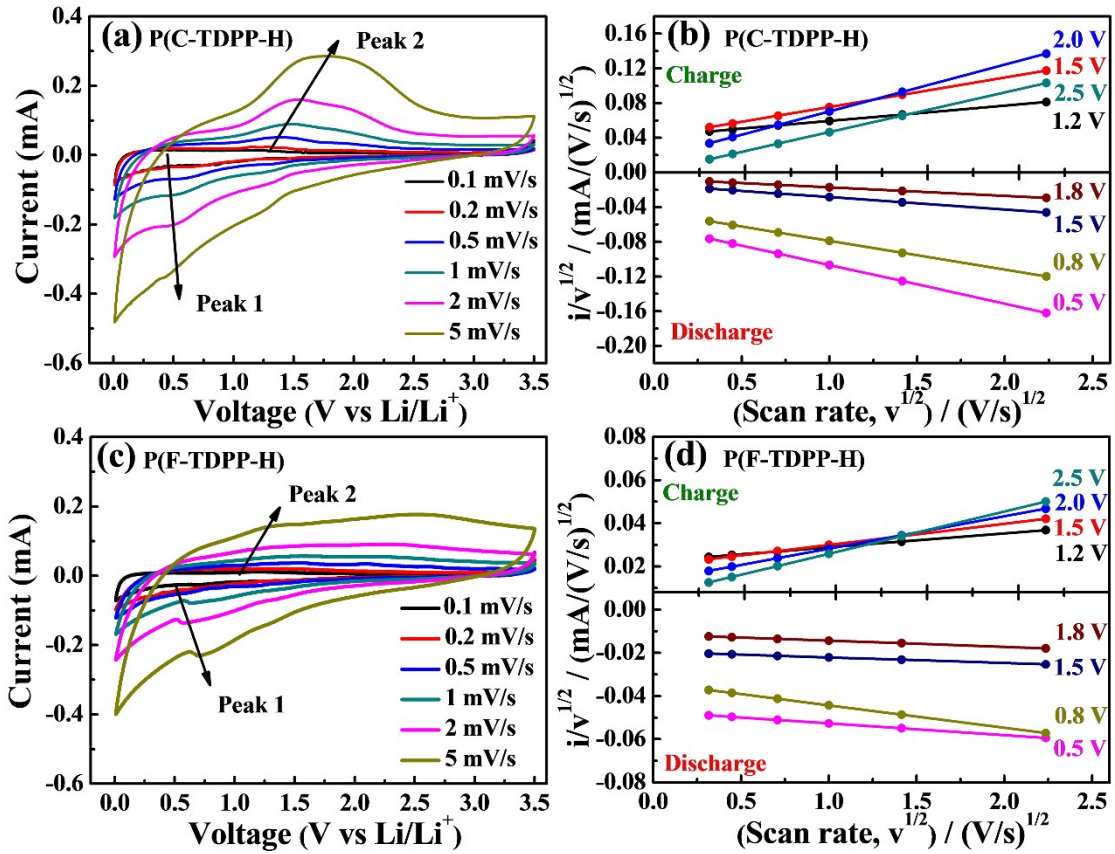
3 Herein, the lithiation/delithiation of the polymer electrode is related to the
4 polymerization unit. Each polymerization unit can react with lithium-ions, and its
5 relative mass fraction (M) is equivalent to the M of the polymerization unit, P(C-TDPP-
6 TA) (M is about 929 g mol^{-1}), P(F-TDPP-TA) (M is about 914 g mol^{-1}), P(C-TDPP-H)
7 (M is about 869 g mol^{-1}) and P(F-TDPP-H) (M is about 854 g mol^{-1}). In the four
8 polymer anodes, their capacity depends on the oxidation-reduction reaction of carbonyl
9 groups with lithium-ions at high voltage ($1.0\sim 3.0 \text{ V}$) and relies on the
10 lithiation/delithiation of planar conjugated groups (phenyl, carbazolyl and fluorenyl
11 groups) or heterocyclic groups (pyrrole and thiophene) at low voltage ($0.01\sim 1.0 \text{ V}$).¹⁻³
12 In theory, each π - π conjugated bond of organic anode materials can attract two metered
13 lithium-ions at low voltage ($0.01\sim 1.0 \text{ V}$).^{1,2} Therefore, the theoretical numbers of
14 lithium insertion (n) of the four polymers reported in this study are respectively P(C-
15 TDPP-TA) ($n=28 \text{ mol}$), P(F-TDPP-TA) ($n=28 \text{ mol}$), P(C-TDPP-H) ($n=26 \text{ mol}$) and
16 P(F-TDPP-H) ($n=26 \text{ mol}$). According to Eq. S1, the theoretical specific capacity (C_T)
17 of the four polymer electrodes can be calculated as P(C-TDPP-TA) ($C_T=807.79 \text{ mAh}$
18 g^{-1}), P(F-TDPP-TA) ($C_T=821.05 \text{ mAh g}^{-1}$), P(C-TDPP-H) ($C_T=801.88 \text{ mAh g}^{-1}$) and
19 P(F-TDPP-H) ($C_T=815.97 \text{ mAh g}^{-1}$). Polymers can enhance the insolubility of small
20 organic molecules in order to retain more effective specific capacity during cycling.
21 However, the polymer anode cannot reach the theoretical numbers of lithium insertion
22 because of steric hindrance in actual discharge. P(C-TDPP-TA) anode has the best
23 discharge specific capacity in the four polymer anodes, which is ascribed to the C-N
24 stretching vibration in the carbazole group and the carbonyl functional group in isobutyl
25 acetate enable the polymer electrode to retain more specific capacity during cycling.

26
27
28
29
30
31
32
33
34
35
36
37
38



1
 2 **Figure S5.** Cyclic voltammogram of (a) P(C-TDPP-TA) and (c) P(F-TDPP-TA) at
 3 different scan rates. Plot of $i(V)/v^{0.5}$ vs. $v^{0.5}$ of (b) P(C-TDPP-TA) and (d) P(F-TDPP-
 4 TA) at selected potentials for discharge (lithiation) and charge (delithiation) scans in
 5 cyclic voltammetry. The plots were used to calculate k_1 (slope) and k_2 (x-intercept) from
 6 $i(V)/v^{0.5} = k_1 v^{0.5} + k_2$.

7
 8
 9
 10
 11
 12



1
2 **Figure S6.** Cyclic voltammogram of (a) P(C-TDPP-H) and (c) P(F-TDPP-H) at
3 different scan rates. Plot of $i(V)/v^{0.5}$ vs. $v^{0.5}$ of (b) P(C-TDPP-H) and (d) P(F-TDPP-H)
4 at selected potentials for discharge (lithiation) and charge (delithiation) scans in cyclic
5 voltammetry. The plots were used to calculate k_1 (slope) and k_2 (x-intercept) from
6 $i(V)/v^{0.5} = k_1 v^{0.5} + k_2$.

7

8

9 **Table S1.** Ionic conductivity of different polymer electrodes calculated by the fitting
10 result of EIS dates.

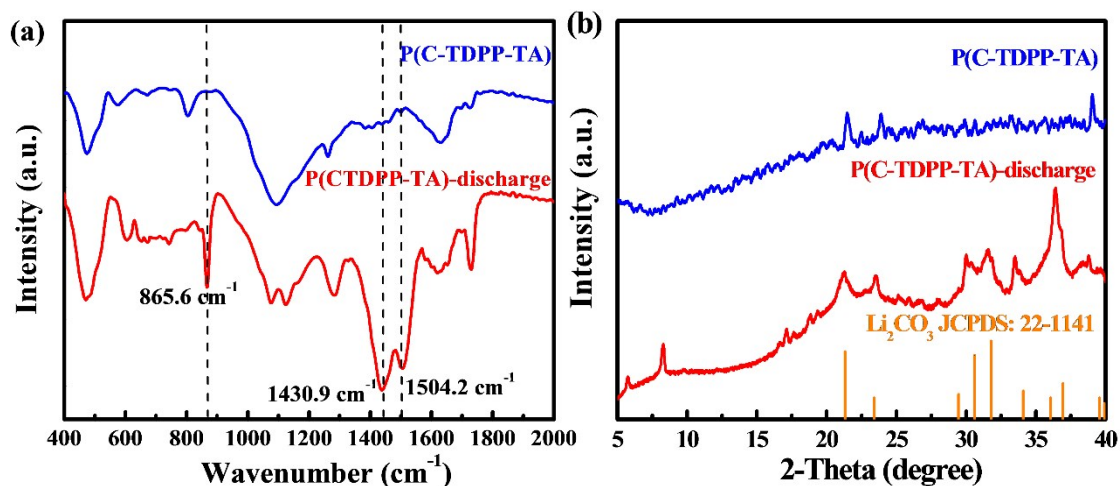
Electrodes	R_s / Ω	R_{ct} / Ω	$\sigma_e/$ ($\times 10^{-3}$ S m $^{-1}$)	Z_w / Ω	$\sigma_i/$ ($\times 10^{-3}$ S m $^{-1}$)	R_{tot} / Ω	$\sigma/$ ($\times 10^{-3}$ S m $^{-1}$)
P(C-TDPP-TA)	3.91	347.10	2.43	209.30	4.08	560.31	1.53
P(F-TDPP-TA)	5.81	577.10	1.47	1145.0	0.75	1727.91	0.49
P(C-TDPP-H)	3.43	236.60	3.56	154.0	5.55	394.03	2.17
P(F-TDPP-H)	6.89	171.30	4.80	127.80	6.68	305.99	2.79

11 * The thickness of electrode (l) is 100 μm and the surface area of electrode (S) is 1.17 cm^2 .

12

13

14



1

2 **Figure S7.** Comparison of (a) FT-IR spectra and (b) XRD patterns of P(C-TDPP-TA)
 3 electrode before and after the first-discharge at 100 mA g⁻¹.

4

5 In Figure S7 (a), a layer of Li₂CO₃ is formed on the surface of the P(C-TDPP-TA)
 6 electrode after the first-discharge, which is corresponding to the vibration peaks at
 7 865.6, 1430.9 and 1504.2 cm⁻¹. In addition, the crystal plane of Li₂CO₃ is also
 8 characterized on the surface of the P(C-TDPP-TA) electrode after the first-discharge as
 9 shown in Figure S7 (b), which further proves the formation of Li₂CO₃ layer.

10

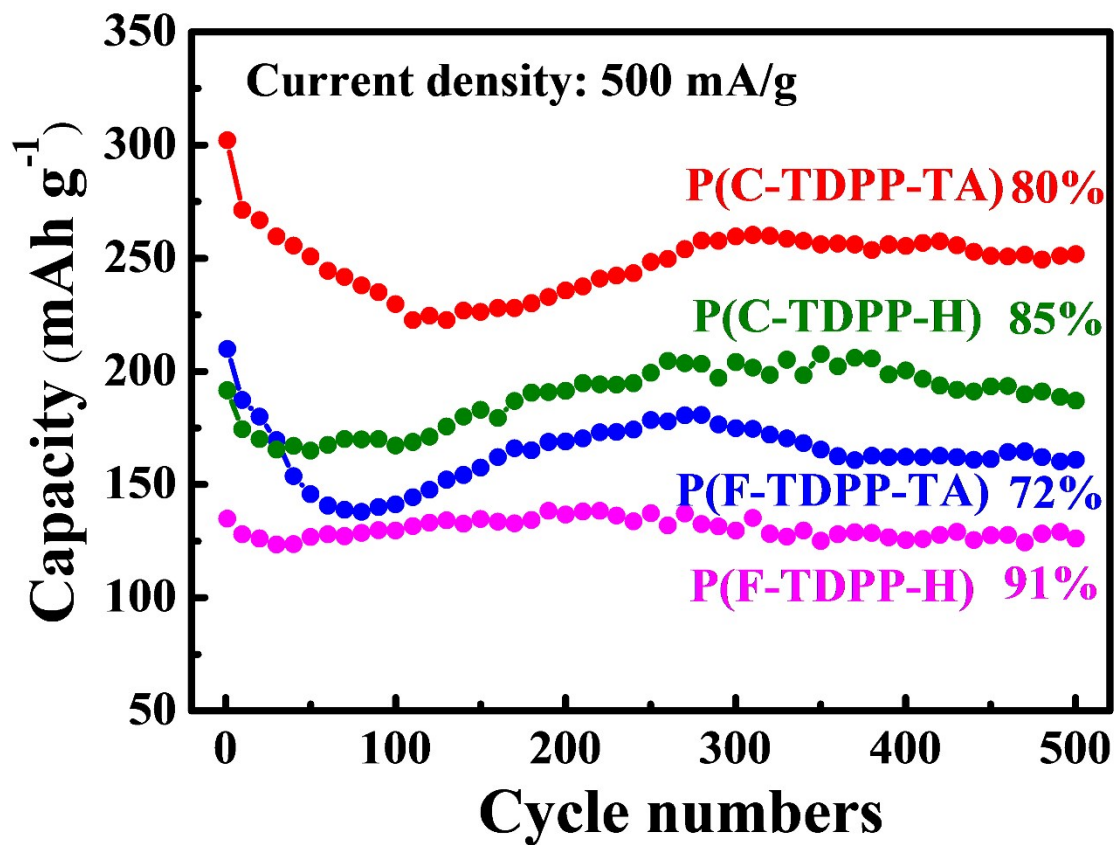
11

12

13

14

15



1

2 **Figure S8.** Comparison of cycling performance of four TDPP-based polymer
 3 electrodes at a current density of 500 mA g⁻¹ for 500 cycles.

4

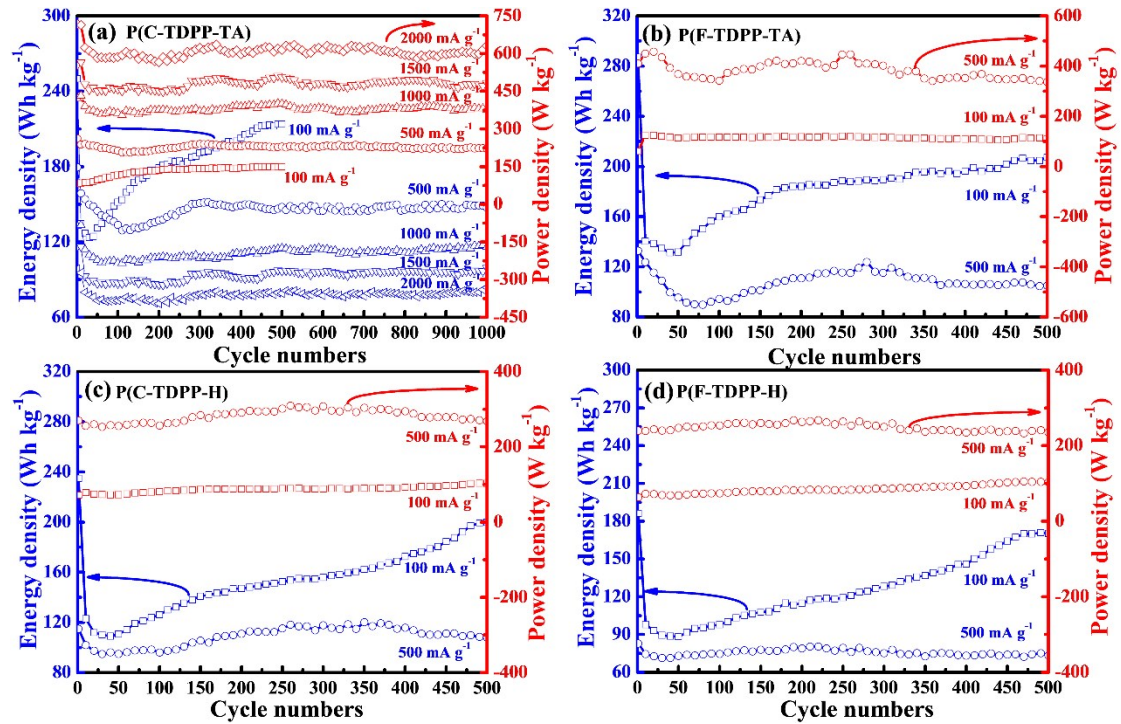
5

6

7

8

9



1

2 **Figure S9.** Energy and power density of (a) P(C-TDPP-TA), (b) P(F-TDPP-TA), (c)
 3 P(C-TDPP-H) and (d) P(F-TDPP-H) at different current densities.

4

5 The energy density (E) and power density (P) of anode materials for lithium-ion
 6 batteries conform to the following formula:

$$7 \quad E = \Delta V \cdot C_m \quad (Wh \cdot kg^{-1}) \quad \text{(Eq.S2)}$$

$$8 \quad P = 3600E / \Delta t \quad (W \cdot kg^{-1}) \quad \text{(Eq.S3)}$$

9 where ΔV (V) represents discharge voltage platform, C_m (Ah kg^{-1}) represents discharge
 10 specific capacity and Δt (s) represents discharge time.

11

12

13

14

15

16

17

18

19

20

21

1 **Table S2.** Impedance parameters derived using equivalent circuit model for the P(C-
2 TDPP-TA) electrode performed after different cycles.

Electrodes	R_s (Ω)	R_f (Ω)	Q_1 (μF)	η_1	C_1 (μF)	R_{ct} (Ω)	Q_1 (μF)	η_2	C_2 (μF)
P(C-TDPP-TA) (1st)	4.89	29.24	5.39	0.93	7.98	308.6	15.54	0.82	99.87
P(C-TDPP-TA) (5th)	4.76	35.48	5.98	0.92	9.63	377.9	10.23	0.85	43.94
P(C-TDPP-TA) (10th)	4.82	46.44	6.64	0.91	11.81	485.0	9.84	0.84	49.39
P(C-TDPP-TA) (20th)	4.46	63.60	7.52	0.88	17.60	438.7	11.38	0.84	57.62
P(C-TDPP-TA) (50th)	4.40	89.62	6.12	0.87	15.81	330.2	18.86	0.82	128.36
P(C-TDPP-TA) (70th)	4.39	78.97	4.23	0.84	12.92	183.4	48.51	0.83	312.39
P(C-TDPP-TA) (100th)	4.20	40.95	5.46	0.89	10.78	108.6	62.72	0.82	435.35

3

4

5

6 References

- 7 [1] X. Han, G. Qing, J. Sun and T. Sun, *Angew. Chem. Int. Edit.*, 2012, 124 (21): 5237-
8 5241.
- 9 [2] Y. Lu, J. Chen, *Nat. Rev. Chem.*, 2020: 1-16.
- 10 [3] J. Wu, X. Rui, G. Long, W. Chen, Q. Yan and Q. Zhang, *Angew. Chem. Int. Edit.*,
11 2015, 54 (25): 7354-7358.